IEICE Communications Express, Vol.13, No.7, 264–267

ComEX

LETTER

Comparison of nonlinear properties in silica-core and hollow-core fibers

Souya Sugiura[1, a)], **Kai Murakami**[1], **Takeshi Takagi**[2], **Kazunori Mukasa**[2], **and Motoharu Matsuura**[1, 3]

Abstract Hollow-core photonic bandgap fibers exhibit nonlinear properties. In comparison with conventional silica-core optical fibers, we experimentally evaluate whether the hollow-core photonic bandgap fiber has extremely low nonlinearity compared with silica-core optical fibers in terms of stimulated Brillouin scattering and four-wave mixing. A low nonlinearity is useful for high-power optical transmission applications.

Keywords: hollow-core fibers, photonic bandgap fibers, stimulated Brillouin scattering, four-wave mixing

Classification: Optical fiber for communications

1. Introduction

Silica-core optical fibers are widely used in optical fiber communications and have contributed significantly to the expansion of transmission capacity [1]. On the other hand, nonlinear phenomena occurring in the silica core are reported to have various effects on transmitted optical signals, such as signal distortion and input power limitation [2].

Recently, hollow-core fibers (HCFs) with an air core have attracted considerable attention because they can dramatically reduce nonlinearity compared to silica-core optical fibers [3, 4, 5, 6, 7, 8, 9, 10, 11]. In addition dramatically improving the transmission capacity of optical fiber communications, HCFs are extremely advantageous for high-power transmission applications, such as passive optical networks [12] and power-over-fiber [13, 14]. Several demonstration experiments on power transmissions that exceed 1 kW have been reported [15, 16].

Although various types of HCFs have been reported, there are generally two types of HCFs. The former is a photonic bandgap fiber (PBGF) [3, 4, 5, 6, 7] and the latter is a nested anti-resonant nodeless fiber (NANF) [8, 9, 10, 11]. Several experiments have been conducted to demonstrate the ultra-low nonlinearity of these fibers and their utilization [9, 11]. However, compared with conventional silica-core optical fibers, no clear evaluation of the differences in various types of nonlinear effects has been reported.

[1] Graduate School of Informatics and Engineering, University of Electro-Communications, 1-5-1 Chofugaoka, Chofu, Tokyo 182-85858, Japan
[2] Photonics Laboratory, Furukawa Electric Co. Ltd., 20-16 Nobono, Kameyana, Mie, 519-0292, Japan
[3] Graduate School of Science and Technology, Keio University, 3-14-1 Hiyoshi, Kouhoku, Yokohama, Kanagawa, 223-8522, Japan
[a)] s.sugiura@uec.ac.jp

DOI: 10.23919/comex.2024XBL0059
Received March 19, 2024
Accepted April 16, 2024
Publicized May 9, 2024
Copyedited July 1, 2024

In this study, to evaluate the nonlinear properties of the HCFs, we experimentally measured their nonlinear characteristics in terms of stimulated Brillouin scattering (SBS) and four-wave mixing (FWM). To demonstrate the low nonlinearity of the HCFs, their characteristics were compared to those of conventional silica-core single-mode fibers (SMFs). Consequently, we have confirmed the ultra-low nonlinearity of HCFs and conducted that they are useful for high-power and multi-channel transmissions.

2. Stimulated Brillouin scattering (SBS)

Brillouin scattering is a scattering phenomenon caused by acoustic phonons with a narrow-linewidth light injection into optical fibers. In high-power light injection, the transmission power is strictly limited if the power is higher than the Brillouin threshold. The Brillouin threshold power P_{th} under quasi-CW condition is approximately given by [2]

$$P_{\mathrm{th}} = \frac{21A_{\mathrm{eff}}}{g_{\mathrm{B}}L_{\mathrm{eff}}}\left(1 + \frac{\Delta\nu_{\mathrm{p}}}{\Delta\nu_{\mathrm{B}}}\right) \tag{1}$$

where A_{eff} denotes the effective area, L_{eff} is the effective length, g_{B} indicates the Brillouin gain coefficient, $\Delta\nu_{\mathrm{B}}$ is the Brillouin gain bandwidth. These values are determined by the propagating optical fiber itself. On the other hand, $\Delta\nu_{\mathrm{p}}$ indicates the input laser linewidth determined by the light source of input light. For conventional silica-core optical fibers, the value of $\Delta\nu_{\mathrm{B}}$ is approximately 25 MHz [17]. If $\Delta\nu_{\mathrm{p}}$ is much smaller than this value, the P_{th} is calculated by

$$P_{\mathrm{th}} = \frac{21A_{\mathrm{eff}}}{g_{\mathrm{B}}L_{\mathrm{eff}}} \tag{2}$$

However, when $\Delta\nu_{\mathrm{p}}$ is larger than this value, the P_{th} increases with the $\Delta\nu_{\mathrm{p}}$. In other words, for signal transmission with a same optical fiber, P_{th} will vary depending on only the $\Delta\nu_{\mathrm{p}}$ of light source used.

To evaluate and compare the effects of SBS on the SMF and HCF, we measured the input/output power characteristics of these fibers. Figure 1 depicts the experimental setup for evaluating SBS in optical fibers. We used two light sources with different linewidths to compare the degree of SBS for different linewidths. The first was an external-cavity laser diode (ECL) with a linewidth of 80 kHz. The second was an ECL with a linewidth of 50 MHz. The output wavelength of these ECLs was 1550 nm. The laser output was amplified using an erbium-doped fiber amplifier (EDFA), and the amplified spontaneous emission noise was removed using a bandpass filter (BPF) with a 3 dB bandwidth of 0.6 nm. Subsequently, the amplified light was transmitted to the SMF or HCF. In this experiment, we used two types of 1 km

test fibers. The first was a commercially available silica-core standard SMF-28 fiber (Thorlabs, Inc., SMF-28). The mode field diameter (MFD) and transmission loss were 10.4±0.5 μm and 0.18 dB/km at 1550 nm, respectively. The other was a photonic bandgap HCF that employs perturbed resonance for improved single modedness (PRISM) [7], as shown in the inset of Fig. 1. The fiber had a large central air core and six large holes that surrounded the core to achieve single-mode propagation. The effective core area of the central air core was approximately 200 μm^2. The HCF contained SMF-based FC/PC connectors at both ends. The expected fiber transmission loss and connection loss per end were 3.1 dB and 1.1 dB, respectively. The total HCF link loss was 5.3 dB. The power of the transmitted light power was measured using an optical power meter (OPM).

Figure 2 shows the input/output characteristics of the 1 km SMF and HCF transmissions for the two laser linewidths. For the SMF transmission using the 80 kHz linewidth laser, the output power was severely limited by the SBS, and it was observed that the output power did not change as the input power increased when the power exceeded 120 mW. In SMF-28, the values of A_{eff} and g_{B} are shown as approximately 80 μm^2 and 1.3×10^{-11} m^{-1} W^{-1}, respectively [18]. Substituting these values into Eq. (2) yields P_{th} as 129 mW. This means that the calculated threshold power is in good agreement with the experimental result. When the linewidth was increased to 50 MHz to mitigate SBS, the saturated output power increased. However, the output power did not change with an increase in the input power beyond 370 mW. If $\Delta\nu_{\mathrm{p}}$ and $\Delta\nu_{\mathrm{B}}$ substitute 50 MHz and 25 MHz [17] into Eq. (1), respectively, P_{th} is approximately 400 mW. The threshold power also agrees well with the experimental result, further indicating that the power saturation in the input/output power characteristics is owing to SBS induced in the SMF used. For the HCF transmission, linear input/output power characteristics were observed without the output power saturation, even at 80 kHz with a narrow linewidth. The slope of the input/output power characteristics of the HCF transmission was slower than that of the SMF transmission owing to the larger transmission loss in the HCF link. This can be improved if the connection losses to the SMFs with the connector and the losses in the HCF itself are reduced. These results show that the HCFs does not cause SBS in the presented measurement range and demonstrate ultra-low nonlinearity.

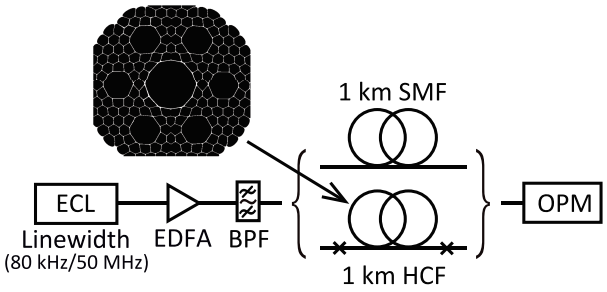

Fig. 1 Experimental setup for evaluating SBS using a 1 km SMF and HCF. ECL: external cavity laser, EDFA: erbium-doped fiber amplifier, BPF: bandpass filter, OPM: optical power meter. Inset shows cross-section of HCF we used.

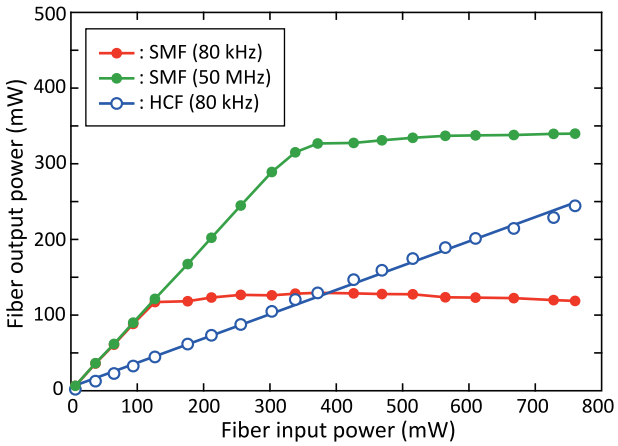

Fig. 2 Input/output power characteristics of 1 km SMF and HCF transmissions for different laser linewidths.

3. Four-wave mixing (FWM)

FWM is an optical parametric effect that occurs during the injection of two or more lights of different wavelengths. The generated FWM components degrade the original signal quality. Therefore, it is crucial to evaluate FWM in multi-channel optical signal transmission. For example, the optical power of the FWM component produced by three input signal powers (P_{i}, P_{j}, and P_{k}) with different wavelengths can be expressed as [19].

$$P_{\mathrm{fwm}} = \eta_{\mathrm{fwm}}(2\gamma L)^2 P_{\mathrm{i}} P_{\mathrm{j}} P_{\mathrm{k}} e^{-\alpha L} \tag{3}$$

where γ is a nonlinear coefficient, α indicates the fiber loss, and L denotes the fiber length. Additionally, η_{fwm} is a measure of the FWM efficiency, which depends on the channel spacing through the phase mismatch determined by the chromatic dispersion in the optical fibers.

Figure 3 shows the experimental setup for evaluating the FWM using the 1 km SMF and HCF. We used four ECLs with a linewidth of 80 kHz as light source. These lights were combined using a 4×1 optical coupler (OC) and amplified using an EDFA. In this experiment, the polarizations of the lights were scrambled without polarization controllers, assuming a real transmission system. The total power input to the test fibers was 23 dBm. After transmission, the transmitted light spectrum was observed using an optical spectrum analyzer (OSA). Among these lights, one ECL output maintained a fixed wavelength of 1552.47 nm, while the other wavelengths were configured with a 50 GHz or 25

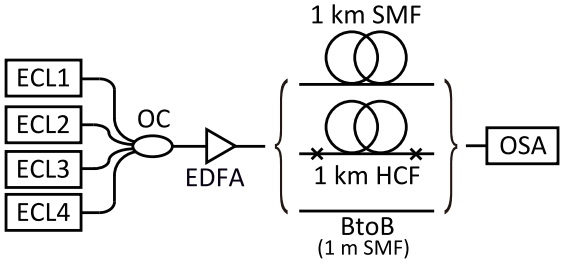

Fig. 3 Experimental setup for evaluating FWM in 1 km SMF, HCF, and back-to-back (BtoB) transmissions. OC: optical coupler, OSA: optical spectrum analyzer.

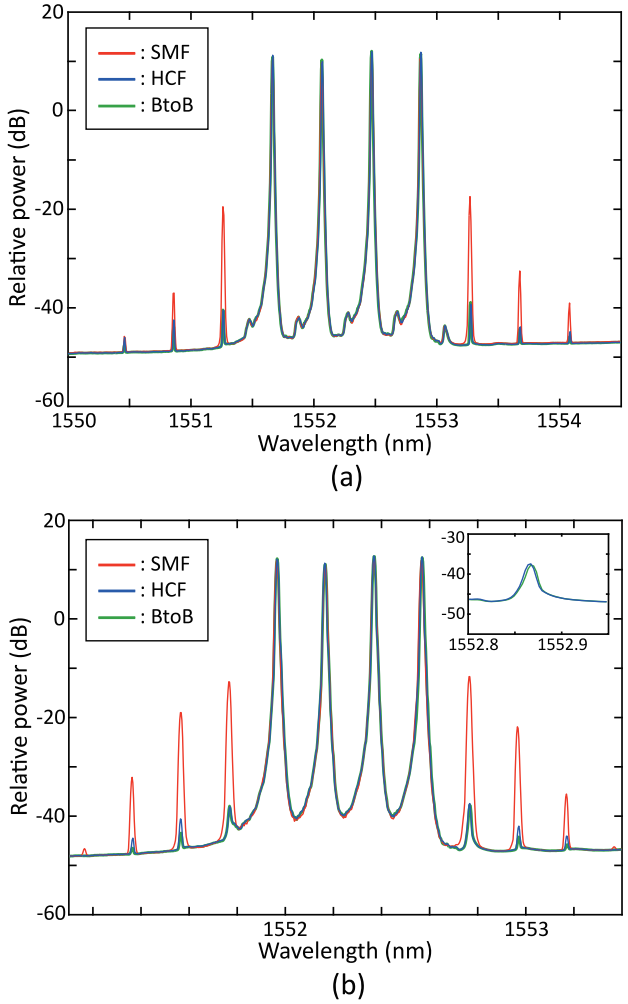

Fig. 4 Output spectra of four-channel transmitted light with (a) 50 GHz and (b) 25 GHz channel spacings in 1 km SMF, HCF and BtoB transmissions. Inset shows output spectrum of extended FWM component on long wavelength side.

GHz channel spacing.

Figure 4 illustrates the output spectra of the 4-channel transmitted lights with 50 GHz and 25 GHz channel spacings in the 1 km SMF (red curve) and HCF (blue curve) transmissions when the total fiber input power was 23 dBm. Notably, the power level was relatively adjusted for the losses in order to provide a clear comparison of FWM occurrences. The spectrum of the SMF transmission has pronounced FWM components, whereas that of the HCF transmission does not have pronounced FWM components. Furthermore, as the channel spacing narrowed from 50 GHz to 25 GHz, the FWM component was found to be more pronounced in the SMF transmission. However, the increase in the FWM component is almost negligible for the HCF transmission. This indicates that the nonlinearity of the HCF is negligible, as shown in Eq. (2). In addition, the spectrum is almost identical to the spectrum of the back-to-back (BtoB) transmission (green curve), which is a direct connection between the EDFA output and the OSA input using a 1 m SMF. The inset of Fig. 4(b) shows the output spectrum of the extended FWM component on the long wavelength side. The peak power difference between the BtoB and HCF transmissions

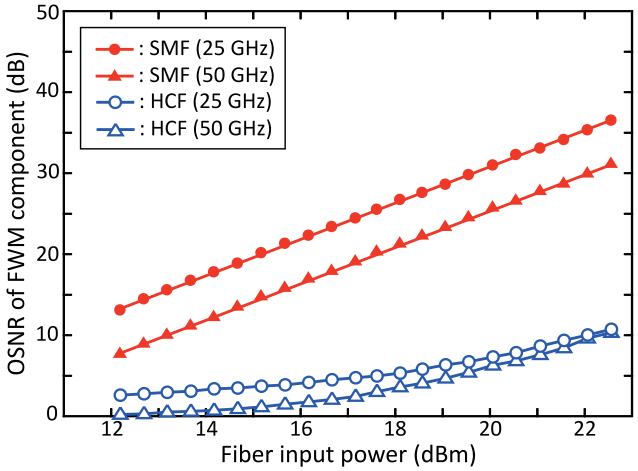

Fig. 5 OSNR of FWM component while changing fiber input power in 1 km SMF and HCF transmissions.

is less than 0.14 dB. This indicates that the FWM components were not induced by the HCF transmission, but by the short SMF link, which comprised the OC, EDFA, and its connected SMFs. These results also show that the HCFs exhibit ultra-low nonlinearity in the case of multi-channel signal transmission.

To evaluate the differences in the FWM components in detail, we measured the optical signal-to-noise ratio (OSNR) of the FWM component power for each channel spacing when the total fiber input power varied. The results are presented in Fig. 5. In the experiment, we measured the OSNR of the FWM component next to the signal on the longest wavelength side of the 4-channel transmitted lights. For a 1 km SMF transmission, the OSNR increased linearly with the fiber input power. Additionally, the OSNR increased as the channel spacing narrowed from 50 GHz to 25 GHz. However, for the HCF transmissions, the increase in the OSNR was not linear and was much smaller than that for the SMF transmission. In addition, at a high fiber input power, a comparable OSNR was observed, regardless of the channel spacing. This was due to the FWM that occurred outside the HCF, as it was almost the same as that for the back-to-back transmissions, as shown in the inset of Fig. 4(b).

4. Conclusion

We experimentally evaluated the nonlinear properties of SBS and FWM in a photonic bandgap-based HCF in detail. Compared with the silica-core SMFs, the results showed that SBS and FWM rarely occurred in the HCFs. The presented ultra-low nonlinearity of the HCFs is advantageous for high-power transmission applications and multi-channel signal transmissions.

Acknowledgments

This work was supported in part by the “Research and Development of Advanced Optical Transmission Technologies for a Green Society” by the Ministry of Internal Affairs and Communications (MIC) (JPMI00316) and the “High-power Analog Radio-over-fiber Technology (HART)” by the Na-

tional Institute of Information and Communications Technology (NICT) (JPJ012368C07101). This research was conducted at the Keio Future Optical Network Open Lab. The authors also appreciate for the technical supports and discussions of OFS.

References

[1] B.J. Puttnam, M. van den Hout, G. Di Sciullo, R.S. Luis, G. Rademacher, J. Sakaguchi, C. Antonelli, C. Okonkwo, and H. Furukawa, "22.9 Pb/s data-rate by extreme space-wavelength multiplexing," Proc. Eur. Conf. Opt. Commun. (ECOC 2023), pp. 1–3, Th.C.2.1, 2023. DOI: 10.1049/icp.2023.2665

[2] G. Agrawal, *Nonlinear Fiber Optics*, Academic Press, New York, 2013. DOI: 10.1016/C2011-0-00045-5

[3] P.J. Roberts, F. Couny, H. Sabert, B.J. Mangan, D.P. Williams, L. Farr, M.W. Mason, A. Tomlinson, T.A. Birks, J.C. Knight, and P.St.J. Russell, "Ultimate low loss of hollow-core photonic crystal fibres," *Opt. Express*, vol. 13, no. 1, pp. 236–244, Jan. 2005. DOI: 10.1364/OPEX.13.000236

[4] M.N. Petrovich, F. Poletti, A. van Brakel, and D.J. Richardson, "Robust single mode hollow core photonic bandgap fiber," *Opt. Express*, vol. 16, no. 6, pp. 4337–4346, March 2008. DOI: 10.1364/OE.16.004337

[5] J.M. Fini, J.W. Nicholson, R.S. Windeler, E.M. Monberg, L. Meng, B. Mangan, A. DeSantolo, and F.V. DiMarcello, "Low-loss hollow-core fibers with improved single-modedness," *Opt. Express*, vol. 21, no. 5, pp. 6233–6242, March 2013. DOI: 10.1364/OE.21.006233

[6] B. Zhu, B.J. Mangan, T. Kremp, G.S. Puc, V. Mikhailov, K. Dube, Y. Dulashko, M. Cortes, Y. lian, K. Marceau, B. Violette, D. Cartsounis, R. Lago, B. Savran, D. Inniss, and D.J. DiGiovanni, "First demonstration of hollow-core-fiber cable for low latency data transmission," Proc. Opt. Fiber Commun. Conf. and Exhibition (OFC 2020), Th4B.3, March 2020. DOI: 10.1364/ofc.2020.th4b.3

[7] K. Mukasa and T. Takagi, "Hollow core fiber cable technologies," *Opt. Fiber Technol.*, vol. 80, Art. 103447, July 2023. DOI: 10.1016/j.yofte.2023.103447

[8] F. Poletti, "Nested antiresonant nodeless hollow core fiber," *Opt. Express*, vol. 22, no. 20, pp. 23807–23828, Oct. 2014. DOI: 10.1364/OE.22.023807

[9] Z. Liu, M.N. Petrovich, D.J. Richardson, F. Poletti, R. Slavik, P. Bayvel, B. Karanov, L. Galdino, J.R. Hayes, D. Lavery, K. Clark, K. Shi, D.J. Elson, and B.C. Thomsen, "Nonlinearity-free coherent transmission in hollow-core antiresonant fiber," *J. Lightw. Technol.*, vol. 37, no. 3, pp. 909–916, Feb 2019. DOI: 10.1109/JLT.2018.2883541

[10] G.T. Jasion, H. Sakr, J.R. Hayes, S.R. Sandoghchi, L. Hooper, E.N. Fokoua, A. Saljoghei, H.C. Mulvad, M. Alonso, A. Taranta, T.D. Bradley, I.A. Davidson, Y. Chen, D.J. Richardson, and F. Poletti, "0.174 dB/km hollow core double nested antiresonant nodeless fiber (DNANF)," Proc. Opt. Fiber Commun. Conf. Exhib. (OFC 2022), pp. 1–3, Th4C.7, 2022. DOI: 10.1364/ofc.2022.th4c.7

[11] X. Zhang, Z. Feng, D. Marpaung, E.N. Fokoua, H. Sakr, J.R. Hayes, F. Poletti, D.J. Richardson, and R. Slavík, "Low-loss microwave photonics links using hollow core fibers," *Light Sci. Appl.*, vol. 11, Art. 213, July 2022. DOI: 10.1038/s41377-022-00908-3

[12] H. Tsuda, "High power optical transmission system using a hollow core optical fiber," *IEICE Tech. Rep.*, PN2023-03, April 2023 (in Japanese).

[13] M. Matsuura, "Recent advancement in power-over-fiber technologies," *Photonics*, vol. 8, no. 8, Art. 8080335, Aug. 2021. DOI: 10.3390/photonics8080335

[14] M. Matsuura, "Power-over-fiber using double-clad fibers," *J. Lightw. Technol.*, vol. 40, no. 10, pp. 3187–3196, May 2022. DOI: 10.1109/JLT.2022.3164566

[15] H.C.H. Mulvad, S. Abokhamis Mousavi, V. Zuba, L. Xu, H. Sakr, T.D. Bradley, J.R. Hayes, G.T. Jasion, E. Numkam Fokoua, A. Taranta, S.-U. Alam, D.J. Richardson, and F. Poletti, "Kilowatt-average-power single-mode laser light transmission over kilometre-scale hollow-core fibre," *Nat. Photon.*, vol. 16, no. 6, pp. 448–453, May 2022. DOI: 10.1038/s41566-022-01000-3

[16] M.A. Cooper, J. Wahlen, S. Yerolatsitis, D. Cruz-Delgado, D. Parra, B. Tanner, P. Ahmadi, O. Jones, M.S. Habib, I. Divliansky, J.E. Antonio-Lopez, A. Schülzgen, and R. Amezcua Correa, "2.2 kW single-mode narrow-linewidth laser delivery through a hollow-core fiber," *Optica*, vol. 10, no. 10, pp. 1253–1259, Oct. 2023. DOI: 10.1364/OPTICA.495806

[17] A. Kobyakov, M. Sauer, and D. Chowdhury, "Stimulated Brillouin scattering in optical fibers," Adv. Opt. Photon., vol. 2, no. 1, pp. 1–59, Jan. 2010. DOI: 10.1364/AOP.2.000001

[18] C.J. Misas, P. Petropoulos, and D.J. Richardson, "Slowing of pulses to c/10 with subwatt power levels and low latency using Brillouin amplification in a bismuth-oxide optical fiber," *J. Lightw. Technol.*, vol. 25, no. 1, pp. 216–221, Jan. 2007. DOI: 10.1109/JLT.2006.887185

[19] G. Agrawal, *Fiber-Optic Communication Systems*, John Willey & Sons, New York, 2010. DOI: 10.1002/9780470918524